

---

# Unpicking Data at the Seams: Understanding Disentanglement in VAEs

---

Carl Allen<sup>1</sup>

## Abstract

Disentanglement, or identifying statistically independent factors of the data, is relevant to much of machine learning, from controlled data generation and robust classification to efficient encoding and improving our understanding of the data itself. Disentanglement arises in several generative paradigms including Variational Autoencoders (VAEs), Generative Adversarial Networks and diffusion models. Recent progress has been made in understanding disentanglement in VAEs, where a choice of *diagonal* posterior covariance matrices is shown to promote mutual orthogonality between columns of the decoder’s Jacobian. We build on this to show how such orthogonality, a geometric property, translates to disentanglement, a statistical property, furthering our understanding of how a VAE identifies independent components of, or disentangles, the data.

## 1. Introduction

Variational Autoencoders (VAEs, Kingma & Welling (2014); Rezende et al. (2014)) and variants, e.g.  $\beta$ -VAE (Higgins et al., 2017) and Factor-VAE (Kim & Mnih, 2018), are often found to *disentangle* latent factors of variation in the data. For example, a trained VAE may generate face images that vary in distinct semantically meaningful ways, such as hair colour or facial expression, as individual latent variables are adjusted. This is both of practical interest, e.g. for controlled generation of synthetic data, and intriguing as it is not knowingly designed into the training algorithm. A similar phenomenon is observed in samples of Generative Adversarial Networks (GANs, Goodfellow et al., 2014), which, in common with VAEs, apply a deterministic neural network function to samples of independently distributed latent variables, producing a *push-forward* distribution.

While disentanglement lacks a firm definition it typically refers to identifying semantically meaningful generative fac-

tors of the data (Bengio et al., 2013). Thus understanding it and how it can arise *seemingly for free* goes to the heart of much of machine learning, from classification to generation, interpretability to identifiability, right down to a fundamental understanding of the data itself. With a better appreciation, we might induce disentanglement more reliably, particularly in domains where we cannot perceive it as readily as we can for images and text.

We focus on disentanglement in VAEs, interest in which has recently piqued due to improved generative quality (e.g. Hazami et al., 2022) and auto-encoders being used in state of the art diffusion models (Rombach et al., 2022; Pandey et al., 2022; Zhang et al., 2022; Yang et al., 2023). Recent works trace the cause of disentanglement in VAEs to the use of *diagonal posterior covariance matrices* (Rolinek et al., 2019; Kumar & Poole, 2020), a common, seemingly innocuous design choice made for computational efficiency. Diagonal covariances are suggested to promote orthogonality between columns of the Jacobian of the decoder, a property linked to disentangled features (Ramesh et al., 2018) and independent causal mechanisms (Gresele et al., 2021).

Extending this work, we first strengthen the “diagonal covariance causes Jacobian orthogonality” argument suggested previously. We then show theoretically how such orthogonality, a geometric property, translates to statistically independent generative factors, or components, in a VAE’s push-forward distribution, which both explains and provides a first clear definition of disentanglement. Specifically, we:

- make precise the link between posterior covariances and the decoder Jacobian, approximated in prior work (§3);
- prove that orthogonality between columns of the decoder Jacobian implies that distinct latent variables manifest as *statistically independent* components of the data distribution (§4);
- establish that disentanglement relates to factorising the push-forward distribution, defined by the prior and decoder, as a product of push-forwards of each latent factor (§4); and
- show that for exponential family likelihoods,  $\beta$  in a  $\beta$ -VAE scales the likelihood’s variance, justifying  $\beta$ ’s role in both disentanglement and “posterior collapse” (§5).

<sup>1</sup>École Normale Supérieure, Paris, France. Correspondence to: <carl.allen@ens.fr>.

## 2. Background

**Disentanglement:** Disentanglement is not a rigorously defined term, but typically refers to identifying salient, semantically meaningful features of the data with distinct latent variables, such that varying a single variable generates data differing in a single aspect (Bengio et al., 2013; Higgins et al., 2017; Ramesh et al., 2018; Rolinek et al., 2019; Shu et al., 2019). We show that disentanglement in a VAE relates to identifying *statistically independent components* of the data, akin to independent component analysis (ICA).

**Variational Autoencoder (VAE):** A VAE is a latent generative model for data  $x \in \mathcal{X} \doteq \mathbb{R}^m$ , that models the data distribution as  $p_\theta(x) = \int_z p_\theta(x|z)p(z)$  with parameters  $\theta$  and latent variables  $z \in \mathcal{Z} \doteq \mathbb{R}^d$ . A VAE is trained by maximising a lower bound (ELBO) on the log likelihood,

$$\int_x p(x) \log p_\theta(x) \geq \int_x p(x) \int_z q_\phi(z|x) \left\{ \log p_\theta(x|z) - \beta \log \frac{q_\phi(z|x)}{p(z)} \right\} \doteq \ell(\theta, \phi), \quad (1)$$

where  $q_\phi(z|x)$  learns to approximate the model posterior  $p_\theta(z|x) \doteq \frac{p_\theta(x|z)p(z)}{p_\theta(x)}$ ; and  $\beta = 1$ . A VAE parameterises distributions by neural networks:  $q_\phi(z|x) = \mathcal{N}(z; e(x), \Sigma_x)$  has mean  $e(x)$  and diagonal covariance  $\Sigma_x$  output by an *encoder* network; and  $p_\theta(x|z)$  is typically of exponential family form with natural parameter  $\theta \doteq d(z)$  defined by a *decoder* network.<sup>1</sup> The prior is commonly a standard Gaussian  $p(z) = \mathcal{N}(z; \mathbf{0}, \mathbf{I})$ . While samples generated by a VAE ( $\beta = 1$ ) often exhibit disentanglement, setting  $\beta > 1$  is found to enhance the effect although often at a cost to generative quality (Higgins et al., 2017; Burgess et al., 2018).

**Probabilistic Principal Component Analysis (PPCA, Tipping & Bishop, 1999)** considers the *linear* latent model

$$x = \mathbf{D}z + \epsilon \quad z \sim p(z) = \mathcal{N}(z; \mathbf{0}, \mathbf{I}) \\ \epsilon \sim p_\sigma(\epsilon) = \mathcal{N}(\epsilon; \mathbf{0}, \sigma^2 \mathbf{I}), \quad (2)$$

with parameters  $\theta = \{\mathbf{D} \in \mathbb{R}^{m \times d}, \sigma \in \mathbb{R}\}$  and noise  $\epsilon \in \mathbb{R}^m$ .<sup>2</sup> The analytical form is known for the posterior,

$$p_\theta(z|x) = \mathcal{N}(z; \frac{1}{\sigma^2} \mathbf{M} \mathbf{D}^\top x, \mathbf{M}), \quad \mathbf{M} = (\mathbf{I} + \frac{\mathbf{D}^\top \mathbf{D}}{\sigma^2})^{-1} \quad (3)$$

and maximum-likelihood solution  $\mathbf{D}_* = \mathbf{U}(\mathbf{S} - \sigma^2 \mathbf{I})^{1/2} \mathbf{R}$ , where  $\mathbf{S} \in \mathbb{R}^{d \times d}$ ,  $\mathbf{U} \in \mathbb{R}^{m \times d}$  contain the largest eigenvalues and corresponding eigenvectors of the data covariance  $\mathbf{X} \mathbf{X}^\top$ ; and  $\mathbf{R} \in \mathbb{R}^{d \times d}$  is orthonormal ( $\mathbf{R}^\top \mathbf{R} = \mathbf{I}$ ). As  $\sigma^2 \rightarrow 0$ ,  $\mathbf{D}_*$  approaches the singular value decomposition (SVD) of data matrix  $\mathbf{X} = \mathbf{U} \mathbf{S}^{1/2} \mathbf{V}^\top \in \mathbb{R}^{m \times n}$ , up to  $\mathbf{V}$ , as in classical PCA. The model is deemed *unidentified* due to

<sup>1</sup>Where Gaussian, a fixed variance parameter  $\sigma^2$  is also specified.

<sup>2</sup>We assume throughout that data is centred, which is equivalent to including a mean parameter (Tipping & Bishop, 1999).

the arbitrary  $\mathbf{R}$ . The solution can also be approximated numerically by maximising the ELBO (Eq. 1) via *expectation maximisation*, i.e. iteratively setting  $q_\phi(z|x)$  to its optimum  $p_\theta(z|x)$  (Eq. 3); and maximising w.r.t.  $\theta$  (PPCA<sup>EM</sup>).

**Linear VAE (LVAE):** A VAE with Gaussian likelihood  $p_\theta(x|z) \doteq \mathcal{N}(x; d(z), \sigma^2 \mathbf{I})$  and a linear decoder  $d(x) = \mathbf{D}x$  learns the same model as PPCA (Eq. 2) and differs to PPCA<sup>EM</sup> only in *approximating* the optimal posterior by  $q_\phi(z|x) = \mathcal{N}(z; \mathbf{E}x, \Sigma)$  rather than stepping directly to it. However, if  $\Sigma$  is *diagonal*, an LVAE breaks the rotational symmetry of PPCA (Lucas et al., 2019) since at optimality

$$\Sigma = \mathbf{M}_* = (\mathbf{I} + \frac{1}{\sigma^2} \mathbf{D}_*^\top \mathbf{D}_*)^{-1} = \sigma^2 \mathbf{R}^\top \mathbf{S}^{-1} \mathbf{R}, \quad (4)$$

(by Eq. 3 and definition of  $\mathbf{D}_*$ ) and diagonality requires  $\mathbf{R} = \mathbf{I}$ , limiting LVAE solutions to  $\mathbf{D}_{\text{LVAE}} = \mathbf{U}(\mathbf{S} - \sigma^2 \mathbf{I})^{1/2}$  (unique up to column permutation and sign). We will see that this direct consequence of diagonal posterior covariance is in fact *disentanglement* in the linear case (§4).

**Decoder Jacobian Orthogonality:** Diagonal posterior covariances have also been proposed as the cause of disentanglement in *non-linear* VAEs, by inducing orthogonality between columns of the decoder’s Jacobian (Rolinek et al., 2019; Kumar & Poole, 2020). The generalised argument of Kumar & Poole (2020) takes the expectation (integrating out  $z$ ) of a *truncated* Taylor expansion of the ELBO, giving a deterministic approximation for each  $x \in \mathcal{X}$  (**det-ELBO**)

$$\ell(x) \approx \log p_\theta(x|z=e(x)) + \frac{1}{2} \mathbf{H}_{e(x)}(x) \odot \Sigma_x \\ - \frac{\beta}{2} (\|e(x)\|^2 + \text{tr}(\Sigma_x) - \log |\Sigma_x| - d), \quad (5)$$

where  $\mathbf{H}_z(x) \doteq (\frac{\partial^2 \log p_\theta(x|z)}{\partial z_i \partial z_j})_{i,j}$  is the Hessian of  $\log p_\theta$  evaluated at  $z \in \mathcal{Z}$ ; and  $\odot$  is the Frobenius (dot) product. Differentiating w.r.t.  $\Sigma_x$  and rearranging gives,

$$\Sigma_x^{-1} \approx \mathbf{I} - \frac{1}{\beta} \mathbf{H}_{e(x)}(x), \quad (6)$$

suggesting that diagonal  $\Sigma_x$  encourages solutions with diagonal  $\mathbf{H}_{e(x)}$ . For Gaussian likelihood  $p_\theta(x|z) = \mathcal{N}(x; \mu \doteq d(z), \sigma^2 \mathbf{I})$ , the chain rule implies  $\mathbf{H}_{e(x)}(x) \approx -\frac{1}{\sigma^2} \mathbf{J}_{e(x)}^\top \mathbf{J}_{e(x)}$ , where  $\mathbf{J}_{z^*} = \frac{d\mu}{dz} \Big|_{z^*}$  is the decoder Jacobian evaluated at  $z^* \in \mathcal{Z}$ , assuming higher decoder derivatives are small almost everywhere, as in ReLU networks or similar (Kumar & Poole, 2020). Eq. 6 thus becomes,

$$\Sigma_x^{-1} \approx \mathbf{I} + \frac{1}{\beta \sigma^2} \mathbf{J}_{e(x)}^\top \mathbf{J}_{e(x)} \quad (7)$$

suggesting that diagonal  $\Sigma_x$  encourages *columns of the decoder Jacobian to be orthogonal*. Such orthogonality is claimed to underpin disentanglement, which is supported empirically: columns of a VAE decoder’s Jacobian are notably orthogonal (Rolinek et al., 2019); and directly encouraging Jacobian column-orthogonality is shown to promote disentanglement (Kumar & Poole, 2020). Our main contribution is to more clearly understand disentanglement and theoretically explain its connection to orthogonality (§4).

### 3. From Diagonal Posterior Covariance to Orthogonality

Understanding how disentanglement follows from optimising the ELBO (Eq. 1) is considered in two steps: **(A)** from the ELBO objective with diagonal posterior covariances to column-orthogonality in the decoder Jacobian; and **(B)** from there to disentanglement. Prior works largely address A and our main focus is B, but before building on it, we state more precisely the relationship in part A approximated in prior work (Rolinek et al., 2019; Kumar & Poole, 2020; Reizinger et al., 2022; Bhowal et al., 2024), cf Eqs. 6 and 7:

$$\Sigma_x^{-1} = \mathbf{I} - \frac{1}{\beta} \mathbb{E}_{q(z|x)}[\mathbf{H}_z(x)] \quad (8)$$

$$\approx \mathbf{I} + \frac{1}{\beta\sigma^2} \mathbb{E}_{q(z|x)}[\mathbf{J}_z^\top \mathbf{J}_z]. \quad (9)$$

Eq. 8 defines *exactly* Gaussian posterior covariances that optimise the ELBO (Oppor & Archambeau, 2009) and Eq. 9 follows analogously to Eq. 7. Having removed an approximation, we see that Eq. 6 holds *in expectation* over posteriors  $q_\phi(z|x)$ , and diagonal  $\Sigma_x$  in Gaussian VAEs encourage decoder Jacobian columns to be *orthogonal in expectation*. While a “looser” relationship than Eq. 6 suggested, Eq. 8 tends to Eq. 6 in the limit as  $\sigma \rightarrow 0$  and posteriors concentrate (note by Eq. 9,  $\sigma^2 \doteq \text{Var}[x|z]$  is proportional to  $\Sigma_x \doteq \text{Var}[z|x]$ , i.e. intuitively, (un)certainly in one variable goes hand in hand with (un)certainly in the other).<sup>3</sup>

It can be seen that optimal posterior covariances for a Gaussian VAE (Eq. 8 dropping  $\beta$  for comparison) generalise the well-known result for the linear case (Eq. 3)

$$\Sigma_{x,\text{VAE}} \approx \left( \mathbf{I} + \frac{1}{\sigma^2} \mathbb{E}_{q(z|x)}[\mathbf{J}_z^\top \mathbf{J}_z] \right)^{-1} \quad (10)$$

$$\Sigma_{\text{PPCA}} = \left( \mathbf{I} + \frac{1}{\sigma^2} \mathbf{D}^\top \mathbf{D} \right)^{-1},$$

(since  $d(z) = \mathbf{D}z$  has Jacobian  $\mathbf{J}_z = \mathbf{D}$ ,  $\forall z \in \mathcal{Z}$ ). In the linear case, diagonal  $\Sigma$  causes right singular vectors of optimal  $\mathbf{D}_*$  (columns of  $\mathbf{R}$  in Eq. 4) to be standard basis vectors (i.e.  $\mathbf{R} = \mathbf{I}$ ); and in VAEs with Gaussian likelihood more generally (“Gaussian VAEs”), diagonal  $\Sigma_x$  promotes orthogonality between columns of  $\mathbf{J}_z$  (in expectation). These constraints reconcile since  $\mathbf{J}_z$  being column-orthogonal and having right singular vectors  $\mathbf{R} = \mathbf{I}$  are equivalent statements. In §4 we show how they relate to disentanglement.

**Linear det-ELBO:** We briefly consider Eq. 5 for an LVAE with optimal posterior covariance  $\Sigma$  (dropping  $\beta$  for clarity),

$$\ell_{\text{LVAE}} = \frac{1}{2} \mathbb{E}_x \left[ -\frac{1}{\sigma^2} \|x - \mathbf{D}\mathbf{E}x\|^2 - \|\mathbf{E}x\|^2 \right] - \log |\mathbf{I} + \frac{1}{\sigma^2} \mathbf{D}^\top \mathbf{D}|. \quad (11)$$

<sup>3</sup>While not the focus of this work, we conjecture: (i) that orthogonality is induced the more that posteriors overlap since areas of overlap are subject to multiple simultaneous orthogonality constraints (see also §5); and (ii) that the “looseness” of the relationship may partly explain why disentanglement is observed variably in practice (e.g. Locatello et al., 2019).

This can be seen as both a deterministic objective for PPCA or a regularised objective for classical PCA that *eliminates unidentifiability due to  $\mathbf{R}$*  (Eq. 4). PCA and its variants are widely studied in terms of optima (Kunin et al., 2019; Bao et al., 2020) and learning dynamics (Saxe et al., 2014; Bao et al., 2020) and this may be of interest to explore further.

### 4. From Orthogonality to Disentanglement

We have seen that diagonal posterior covariances in Gaussian VAEs promote column-orthogonality (in expectation) in the decoder’s Jacobian. The question now is *how does that relate to disentanglement?*

We first consider a linear decoder  $d(z) = \mathbf{D}z$ ,  $\mathbf{D} \in \mathbb{R}^{m \times d}$ , which defines a linear manifold of mean parameters  $\mathcal{M}_f \doteq \{\mu = \mathbf{D}z \mid z \in \mathcal{Z}\}$  with Jacobian  $\mathbf{D}$ . Letting  $\mathbf{U}\mathbf{S}\mathbf{V}^\top$  be the SVD of  $\mathbf{D}$ ,<sup>4</sup> column-orthogonality in the Jacobian implies  $\mathbf{V} = \mathbf{I}$ . Since  $z \sim \mathcal{N}(\mathbf{0}, \mathbf{I})$ , the density over the manifold is Gaussian  $p(\mu) = \mathcal{N}(\mu; \mathbf{0}, \mathbf{D}\mathbf{D}^\top)$ . As for any Gaussian,  $p(\mu)$  factorises as a product of 1-dimensional Gaussian densities  $p(\mu) = \prod_i \mathcal{N}(u_i; 0, \mathbf{S}_{i,i}^2)$  over random variables, or *components*,  $u_i \doteq \mathbf{u}^{i\top} \mu \in \mathbb{R}$  defined by projecting  $\mu$  onto left singular vectors  $\mathbf{u}^i$  of  $\mathbf{D}$  (columns of  $\mathbf{U}$ ). Since  $u_i = \mathbf{u}^{i\top} \mathbf{D}z = \mathbf{S}_{i,i} z_i$ , each  $u_i$  is a function of a distinct *independent* latent variable  $z_i$  and so: (i) the density  $p(\mu)$  over  $\mathcal{M}_f$  factorises as a product of independent densities  $p(u_i)$ ; and (ii) the decoder maps each latent variable  $z_i$  to a distinct  $u_i$ . This means that synthetic data generated by re-sampling dimension  $z_i$ , while  $z_{j \neq i}$  are held constant, differ only in component  $u_i$ , i.e. components  $u_i$  are *disentangled*. This suggests a clearer definition of disentanglement: *as factorising the data distribution into independent components*.

Ideally we would apply an analogous argument to non-linear Gaussian VAEs, but the factorisation of  $p(\mu)$  relies on linearity of  $d$  that does not readily generalise. Our strategy is therefore to reconsider the linear case from a different perspective that does extend to the non-linear case.

Note that, more generally, a Gaussian VAE can be considered to sample  $z \sim p(z)$ , apply the deterministic decoder function  $\mu = d(z)$  and add element-wise noise,  $x = \mu + \sigma\epsilon$ . The last step contributes no structure, serving only as “blur” and is typically omitted when generating synthetic data such as images. Samples are thus drawn from the *push-forward distribution* of mean parameters  $p(\mu)$  over a  $d$ -dimensional manifold embedding in  $\mathbb{R}^m$  defined by the decoder (as in the linear case). We assume throughout that  $\sigma$  is sufficiently well estimated or negligible and focus on this push-forward distribution over mean parameters to understand the implications of Jacobian column-orthogonality.

<sup>4</sup>Note the change to prior notation where we took the SVD of  $\mathbf{X}$ .

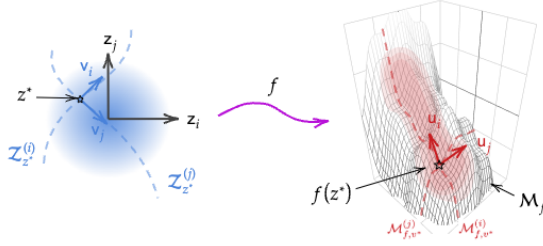


Figure 1. For continuous  $f : \mathcal{Z} \rightarrow \mathcal{X}$  differentiable at  $z^* \in \mathcal{Z}$  with Jacobian  $\mathbf{J}_{z^*}$ ,  $f$  defines a manifold  $\mathcal{M}_f \subseteq \mathcal{X}$ .  $\mathbf{z}_i, \mathbf{z}_j$  denote standard basis vectors in  $\mathcal{Z}$ . Right singular vectors  $\mathbf{v}^i$  of  $\mathbf{J}_{z^*}$  (solid blue) map to left singular  $\mathbf{u}^i$  at  $f(z^*) \in \mathcal{X}$  (solid red). Paths  $\mathcal{V}_{z^*}^i \subseteq \mathcal{Z}$  following right singular vectors at each point (dashed blue) map to paths  $\mathcal{M}_{f,z^*}^i$  over  $\mathcal{M}_f$  along left singular vectors (dashed red).

#### 4.1. Notation and Preliminary Lemmas

For  $\mathcal{Z} = \mathbb{R}^d$ ,  $\mathcal{X} = \mathbb{R}^m$ ,  $d \leq m$  and a continuous function  $f : \mathcal{Z} \rightarrow \mathcal{X}$  differentiable at  $z \in \mathcal{Z}$ , let  $\mathbf{J}_z$  denote the Jacobian of  $f$  evaluated at  $z$  and  $\mathbf{J}_z = \mathbf{U}\mathbf{S}\mathbf{V}^\top$  be its SVD ( $\mathbf{U}^\top\mathbf{U} = \mathbf{I}$ ,  $\mathbf{V}^\top\mathbf{V} = \mathbf{V}\mathbf{V}^\top = \mathbf{I}$ ). Let  $\mathbf{u}^i, \mathbf{v}^i, s^i$  denote the  $i^{\text{th}}$  left and right singular vectors (columns of  $\mathbf{U}, \mathbf{V}$ ) and singular values ( $S_{i,i}$ ), respectively.<sup>5</sup>  $f$  defines a  $d$ -dimensional manifold  $\mathcal{M}_f = \{f(z) \mid z \in \mathcal{Z}\}$  embedded in  $\mathcal{X}$  (See Figure 1). Singular vectors  $\{\mathbf{v}^i\}_i, \{\mathbf{u}^i\}_i$  define orthonormal bases for  $\mathcal{Z}$  at  $z$  and for the tangent space to  $\mathcal{M}_f$  at  $x = f(z)$ .

We consider a broader class of functions than fully differentiable that allows  $f$  to be piece-wise linear.

**Definition 4.1.** A function  $f : \mathcal{Z} \rightarrow \mathcal{X}$  is *quasi-differentiable* if it is continuous and differentiable almost everywhere.

**Definition 4.2.** A quasi-differentiable function  $f : \mathcal{Z} \rightarrow \mathcal{X}$  is *V-continuous* if right singular value matrix  $\mathbf{V}_z$  of Jacobian  $\mathbf{J}_z$  is continuous w.r.t.  $z$  (e.g.  $\mathbf{V}_z$  may be constant  $\forall z \in \mathcal{Z}$ ).

Considering the directional derivative  $\mathbf{J}_z \mathbf{v}^i = \mathbf{U}\mathbf{S}\mathbf{V}^\top \mathbf{v}^i = s^i \mathbf{u}^i$ , shows that a small perturbation by right singular vector  $\mathbf{v}^i$  at  $z \in \mathcal{Z}$  translates under  $f$  to a small perturbation in  $\mathbf{u}^i$  at  $f(z) \in \mathcal{M}_f$ . Intuitively, by extension, a path that follows  $\mathbf{v}^i$  at each point in  $\mathcal{Z}$  maps to a path following  $\mathbf{u}^i$  over the manifold in  $\mathcal{X}$ . To formalise this, we show that “ $i^{\text{th}}$ ” singular vectors can be well defined since columns of an SVD can be permuted to give another valid SVD.

**Lemma 4.3.** If  $f : \mathcal{Z} \rightarrow \mathcal{X}$  is injective and V-continuous, defining  $\mathbf{V}_{z^*}$  for any  $z^* \in \mathcal{Z}$  uniquely defines  $\mathbf{V}_z, \forall z \in \mathcal{Z}$ .

*Proof (sketch, see Appendix A.1).* Since  $\mathbf{V}_z$  is continuous w.r.t.  $z$ , for any  $z^{**} \in \mathcal{Z}$ ,  $\mathbf{V}_z$  converges to the same limit over any path from  $z^*$  to  $z^{**}$ , uniquely defining  $\mathbf{V}_{z^{**}}$ .  $\square$

Herein, we assume  $\mathbf{V}$  is fixed for some  $z^* \in \mathcal{Z}$ , thus ordering of  $\mathbf{v}^i$ , and by implication  $\mathbf{u}^i$  and  $s^i$ , is well-defined and paths over  $i^{\text{th}}$  singular vectors can be defined.

<sup>5</sup>We often omit  $z$  subscripts from  $\mathbf{U}, \mathbf{S}, \mathbf{V}$  to lighten notation.

**Definition 4.4.** If  $f : \mathcal{Z} \rightarrow \mathcal{X}$  is injective and V-continuous, for  $z^* \in \mathcal{Z}$ ,  $t^* \in \mathbb{R}$  let  $z^i(t^*) \doteq z^* + \int_0^{t^*} \mathbf{v}^i dt \in \mathcal{Z}$ , where  $\mathbf{v}^i$  is the  $i^{\text{th}}$  right singular vector at  $z^i(t)$ . The set  $\mathcal{V}_{z^*}^i \doteq \{z^i(t) \mid t \in \mathbb{R}\} \subseteq \mathcal{Z}$  defines the  $i^{\text{th}}$  *singular vector path*, a continuous path in  $\mathcal{Z}$  through  $z^*$  following  $i^{\text{th}}$  right singular vectors  $\mathbf{v}^i$  of  $\mathbf{J}_z$ .

**Lemma 4.5 (Data seams).** Let  $f : \mathcal{Z} \rightarrow \mathcal{X}$  be injective and V-continuous with manifold  $\mathcal{M}_f \subseteq \mathcal{X}$ ,  $z^* \in \mathcal{Z}$  and  $\mathcal{V}_{z^*}^i$  the  $i^{\text{th}}$  singular vector path through  $z^*$ . The image  $\mathcal{M}_{f,z^*}^i \subseteq \mathcal{M}_f$  of  $\mathcal{V}_{z^*}^i$  under  $f$  is a path over  $\mathcal{M}_f$  through  $f(z^*)$  following left singular vectors  $\mathbf{u}^i$  of  $\mathbf{J}_z$  (see Figure 1).

*Proof (sketch, see Appendix A.1).* Follows from the fundamental theorem of calculus and that the Jacobian maps right singular vectors to left singular vectors:  $\mathbf{J}_z \mathbf{v}^i = s^i \mathbf{u}^i$ .  $\square$

Lemma 4.5 is central to our main claims since density over each singular vector path is mapped separably under  $f$ .

**Definition 4.6 (push-forward distribution).** For a function  $f : \mathcal{Z} \rightarrow \mathcal{X}$  and prior distribution  $p(z)$  over  $\mathcal{Z}$ , the *push-forward distribution* is defined implicitly over  $\{x = f(z) \mid z \sim p(z)\} \subseteq \mathcal{X}$  with density

$$p_f^\#(x = f(z)) = p(z) |\mathbf{J}_z|^{-1} = p(z) \prod_i |s^i|^{-1}. \quad (12)$$

**Assumptions:**

**A#1.** Latent variables  $z_i$  are independent standard normal,  $p(z) = \prod_{i=1}^d \mathcal{N}(z_i; 0, 1)$ .<sup>6</sup>

**A#2.**  $f : \mathcal{Z} \rightarrow \mathcal{X}$  is injective and quasi-differentiable.

Note that under A#2,  $f$  is bijective between  $\mathcal{Z}$  and  $\mathcal{M}_f$ ; and  $\mathbf{J}_z$  has full-rank where defined.

#### 4.2. Linear $f$

We now revisit the linear case  $f(z) = \mathbf{D}z$  (satisfying A#2) where  $\mathcal{M}_f$  is a  $d$ -dimensional subspace that defines the mean parameters of the PPCA/LVAE model.

**Theorem 4.7 (Linear disentanglement).** Under A#1, for a linear function  $f : \mathcal{Z} \rightarrow \mathcal{X}$ ,  $f(z) = \mathbf{D}z$  the push-forward distribution  $p_f^\#(x)$  factorises as a product of statistically independent components in  $\mathcal{X}$ . Lines in  $\mathcal{Z}$  following right singular vectors of  $\mathbf{D}$ , corresponding to independent  $z_i$ , map to lines in  $\mathcal{X}$  following left singular vectors of  $\mathbf{D}$  corresponding to statistically independent components.

*Proof (sketch, see Appendix A.2).* In general, the Jacobian of a function may vary over  $\mathcal{Z}$ , but for linear  $f$ ,  $\mathbf{J}_z = \mathbf{D}$  is constant  $\forall z \in \mathcal{Z}$ , as are its singular vectors and values (hence  $f$  is V-continuous). Thus,  $\{\mathbf{v}^i\}_i$  define a *global* basis for  $\mathcal{Z}$  (termed the **V-basis**). Any  $z \in \mathcal{Z}$  can be considered in the **V-basis** as  $v \doteq \mathbf{V}^\top z$  with co-ordinates  $v_i \doteq \mathbf{v}^{i\top} z$ , and sampling  $z \sim p(z)$  can be interpreted as sampling  $v \sim p(v)$

<sup>6</sup>Since A#1 is assumed throughout, we drop subscript  $p$  from  $p_f^\#$ .



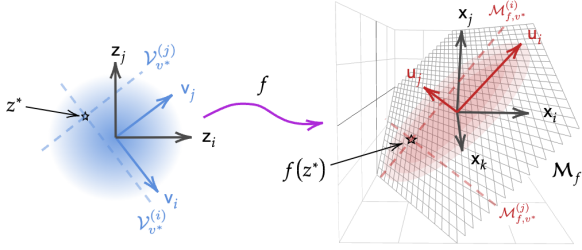


**Figure 2. Transforming Gaussian density under linear  $f$**  (manifold  $\mathcal{M}_f \subseteq \mathcal{X}$ ): Lines  $\mathcal{V}_{z^*}^i \subseteq \mathcal{Z}$  (dashed blue) pass through  $z^*$  parallel to right singular vectors  $v^i$  of Jacobian  $\mathbf{J}_{z^*}$  (solid blue). The image of each  $\mathcal{V}_{z^*}^i$  is a line  $\mathcal{M}_{f,z^*}^i \subseteq \mathcal{M}_f$  (dashed red) passing through  $f(z^*)$  parallel to left singular vectors  $u^i$  of  $\mathbf{J}_{z^*}$  (solid red). Independent marginal distributions over  $\mathcal{V}_{z^*}^i$ ,  $p(v^*) = \prod_i p(v_i^*)$  are “pushed forward” under  $f$  to independent marginal distributions  $p_{f,z^*}^i$  over  $\mathcal{M}_{f,z^*}^i$  that factorise the push-forward distribution over the manifold:  $p_f^\#(x) = \prod_i p_{f,z^*}^i(x)$ .

where  $p(v) = |\mathbf{V}|^{-1}p(z) = p(z)$  (since the basis change is orthonormal). By rotational symmetry of the Gaussian  $p(z)$ ,  $p(v) = \prod_i p(v_i)$ , where  $p(v_i) = \mathcal{N}(v_i, 0, 1)$ , i.e.  $v_i$  are samples of standard normal random variables  $v_i$ , as  $z_i$  are in the standard basis. Importantly,  $p_f^\#$  factorises in the  $\mathbf{V}$ -basis:

$$p_f^\#(x) = p(z) \prod_i |s^i|^{-1} = \prod_i |s^i|^{-1} p(v_i), \quad (13)$$

and each factor  $|s^i|^{-1}p(v_i)$ , or component, is a function of a distinct latent variable  $v_i$ , hence they are independent.

Given  $z^* \in \mathcal{Z}$ , varying a single co-ordinate  $v_i$  in the  $\mathbf{V}$ -basis defines lines  $\mathcal{V}_{z^*}^i \subset \mathcal{Z}$  parallel to  $v^i$  (dashed blue, Figure 2) with marginal distribution over  $z \in \mathcal{V}_{z^*}^i$  given by  $p(v_i)$  (defined above, recall  $v_i \doteq \mathbf{V}^\top z$ ). Thus, any  $z \in \mathcal{Z}$  lies at the intersection of lines  $\mathcal{V}_{z^*}^i$  and  $p(z)$  factorises as a product of marginal densities over those lines. Eq. 13 suggests that the density over the manifold factorises similarly if factors  $|s^i|^{-1}p(v_i)$  define probability distributions. Of course, the Gaussian densities over  $\mathcal{V}_{z^*}^i$  map to Gaussian densities in  $\mathcal{X}$  under linear  $f$ , but we do not want to use linearity of  $f$ .

Each  $\mathcal{V}_{z^*}^i$  describes a singular vector path (Definition 4.4), thus, by Lemma 4.5, its image is a line  $\mathcal{M}_{f,z^*}^i \subseteq \mathcal{M}_f$  parallel to  $u^i$  (dashed red, Figure 2). It can be shown that the marginal density over each  $\mathcal{V}_{z^*}^i$  maps to marginal density  $p_{f,z^*}^i$  over  $\mathcal{M}_{f,z^*}^i$  given by the respective term in Eq. 13, i.e.  $p_{f,z^*}^i(x) = |s^i|^{-1}p(v_i)$  for  $x = f(z) \in \mathcal{M}_{f,z^*}^i$ . This is proved either by marginalising  $p_f^\#(x)$  (Eq. 13) over  $\mathcal{M}_{f,z^*}^i$ , or by considering the the push-forward of the marginal density over  $\mathcal{V}_{z^*}^i$  under  $f$  restricted to a univariate map  $\mathcal{V}_{z^*}^i \rightarrow \mathcal{M}_{f,z^*}^i$ . Thus, Eq. 13 factorises as

$$p_f^\#(x) = \prod_i p_{f,z^*}^i(x). \quad (14)$$

□

To summarise, the proof of Theorem 4.7 unpicks how density maps under  $f$  from  $\mathcal{Z}$  to  $\mathcal{X}$ . The SVD of  $\mathbf{J}_z$  defines how marginal densities along each singular vector  $v^i$  in  $\mathcal{Z}$  map to the respective singular vector  $u^i$  in  $\mathcal{X}$  (the Jacobian of each 1-dimensional mapping given by singular value  $s^i$ ). This doesn’t rely on properties of  $p(z)$ , but if marginal densities over  $\mathcal{V}_z^i$  are independent, as the case for Gaussian  $p(z)$ , then each marginal in  $\mathcal{Z}$  is “pushed-forward” to an independent marginal density over  $\mathcal{M}_{f,z}^i$  in  $\mathcal{X}$ . Hence, just as  $p(z)$  factorises in  $\mathcal{Z}$ , the density  $p(x = f(z))$  of its image on the manifold factorises as a product of marginal push-forward densities. Densities over  $\mathcal{M}_{f,z^*}^i$  can be considered probability distributions over implicit independent random variables, or components, in  $\mathcal{X}$ .

*Remark 4.8.* The probability density over each  $\mathcal{V}_{z^*}^i \subseteq \mathcal{Z}$  is a standard Gaussian  $\mathcal{N}(v; 0, 1)$ . The density over each  $\mathcal{M}_{f,z}^i \subseteq \mathcal{X}$  is Gaussian  $p_{f,z}^i(f(z)) = |s^i|^{-1}p(z_i) = \mathcal{N}(x; 0, (s^i)^2)$  (as known previously using linearity of  $f$ ).

*Remark 4.9.* By considering  $x$  in a (local)  $\mathbf{U}$ -basis  $u \doteq \mathbf{U}^\top x$ , similarly to  $v \doteq \mathbf{V}^\top z$ , the SVD of the Jacobian  $\mathbf{J}_z = \mathbf{U}\mathbf{S}\mathbf{V}^\top$  can be interpreted in terms of the chain rule  $\mathbf{J}_z = \frac{\partial x}{\partial u} \frac{\partial u}{\partial v} \frac{\partial v}{\partial z}$ ; where  $\mathbf{U}, \mathbf{V}^\top$  transform the basis in each domain and  $\mathbf{S} = \frac{\partial u}{\partial v}$  is the Jacobian of the map  $v \mapsto u$  in which only respective dimensions interact:  $\frac{\partial u_i}{\partial v_j} = \{s^i \text{ if } i = j; 0 \text{ otherwise}\}$ .

*Remark 4.10.* Right singular vectors  $\mathbf{V}$  transform from the standard basis to a *natural* basis for  $\mathcal{Z}$ . The standard basis has no effect on  $p(x)$  so  $\mathbf{V}$  can not be recovered and PPCA is identified if  $\mathbf{U}\mathbf{S}$  is recovered.

**Corollary 4.11 (LVAE identifiability).** *For  $n$  data samples generated under the model in Eq. 2 (PPCA model), in the limit  $n \rightarrow \infty$ , an LVAE identifies statistically independent components of the data and the decoder maps latent variables to distinct components. If singular values of ground truth  $\mathbf{D}$  are distinct, the model is uniquely identified (up to permutation and sign).*

*Proof (sketch, see Appendix A.3).* If the model has ground truth  $\mathbf{D} = \mathbf{U}\mathbf{S}\mathbf{V}^\top$ , an optimal LVAE learns  $\mathbf{D}_{\text{LVAE}} \doteq \mathbf{U}\mathbf{S}$ , i.e.  $\mathbf{V}_{\text{LVAE}} = \mathbf{I}$  and right singular vectors of  $\mathbf{D}_{\text{LVAE}}$  are standard basis vectors  $z^i$ . By Lemma 4.5,  $\mathbf{D}_{\text{LVAE}}$  maps a path  $\mathcal{V}_z^i$  following  $z^i$  (i.e. by varying co-ordinate  $z_i$ ) to a path  $\mathcal{M}_{f,z}^i$  in  $\mathcal{X}$  following singular vector  $u^i$ , which correspond to independent components by Theorem 4.7. Identifiability follows from uniqueness of the SVD for distinct singular values up to known symmetries. □

Relating this to our initial consideration of the linear case where the Gaussian distribution over mean parameters was known to factorise into independent Gaussians, Corollary 4.11 proves that an LVAE decoder maps independent latent dimensions  $z_i$  to each factor.

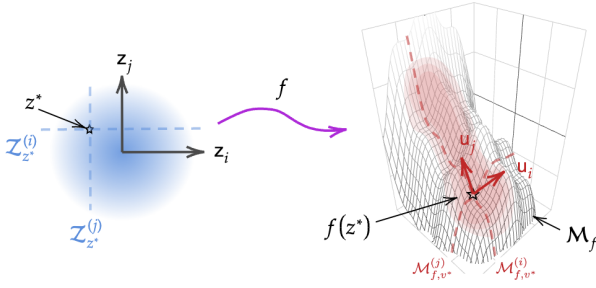


**Figure 3. Transforming Gaussian density under non-linear  $f$  with column-orthogonal Jacobian  $J_{z^*}$**  (manifold  $\mathcal{M}_f \subseteq \mathcal{X}$ ): Lines  $\mathcal{V}_{z^*}^i \subseteq \mathcal{Z}$  (dashed blue) pass through  $z^*$  parallel to (constant) right singular vectors  $v^i$  of  $J_{z^*}$  (solid blue). The image of each  $\mathcal{V}_{z^*}^i$  is a submanifold  $\mathcal{M}_{f,z^*}^i \subseteq \mathcal{M}_f$  (dashed red red) passing through  $f(z^*)$  parallel to left singular vectors  $u^i$  of  $J_{z^*}$  (solid red). Independent marginal distributions over  $\mathcal{V}_{z^*}^i$ ,  $p(v^*) = \prod_i p(v_i^*)$  are "pushed forward" under  $f$  to independent marginal distributions  $p_{f,z^*}^i$  over  $\mathcal{M}_{f,z^*}^i$  that factorise the push-forward distribution over the manifold:  $p_f^\#(x) = \prod_i p_{f,z^*}^i(x)$ .

### 4.3. Non-linear $f$ , column-orthogonal Jacobian

Importantly, the proof of [Theorem 4.7](#) for the linear case does not rely on linearity of  $f$  and we now follow a similar argument for  $f$  that may be non-linear, assuming

**A#3.** Columns of the Jacobian  $J_z$  are mutually orthogonal, i.e.  $\frac{\partial x}{\partial z_i}^\top \frac{\partial x}{\partial z_j} = 0, i \neq j$ ; equivalently  $V_z = I, \forall z \in \mathcal{Z}$ .

**Theorem 4.12 (Non-linear disentanglement).** *Under [A#1-3](#), the push-forward distribution  $p_f^\#$  factorises as a product of statistically independent components in  $\mathcal{X}$  ([Eq. 16](#)). Lines in  $\mathcal{Z}$  following standard basis vectors corresponding to independent latent variables are mapped to sub-manifolds in  $\mathcal{X}$  following left singular vectors of the Jacobian  $J_z$  that correspond to statistically independent components.*

*Proof (sketch, see [Appendix A.4](#)).* Note that [A#2](#) and [A#3](#) imply  $f$  is  $V$ -continuous. We follow the same argument as for [Eq. 12](#) with  $V_z = I, \forall z \in \mathcal{Z}$ , to reach

$$p_f^\#(f(z)) = |J_z|^{-1} p(z) = \prod_i |s^i|^{-1} p(z_i) \quad (15)$$

where  $p(z_i) = \mathcal{N}(z_i; 0, 1)$  is the distribution over coordinate  $z_i$  in the standard basis. Singular vector paths  $\mathcal{Z}_{z^*}^i \subset \mathcal{Z}$  through a point  $z^* \in \mathcal{Z}$  ([Figure 3](#), dashed blue) are parallel to standard basis-vectors  $z^i$  (since  $V = I$ ) with marginal density given by  $p(z_i)$ . Hence  $p(z)$  again factorises over the marginal densities of  $\mathcal{Z}_{z^*}^i$  passing through it. By [Lemma 4.5](#), the image of  $\mathcal{Z}_{z^*}^i$  is a submanifold  $\mathcal{M}_{f,z^*}^i \subseteq \mathcal{M}_f$  through  $f(z^*)$  (dashed red) following left singular vectors  $u^i$  (solid red). The marginal density  $p_{f,z^*}^i(x)$  over  $x = f(z) \in \mathcal{M}_{f,z^*}^i$  is not known analytically in general, but is described by the factors of [Eq. 15](#):  $p_{f,z^*}^i(x) = |s^i|^{-1} p(v_i)$ , which are again independent (as in the linear case).

Thus [Eq. 15](#) factorises exactly as before

$$p_f^\#(x) = \prod_i p_{f,z}^i(x), \quad (16)$$

into statistically independent components, supported on sub-manifolds  $\mathcal{M}_{f,z}^i$  passing through  $x = f(z)$ .  $\square$

**Remark 4.13.** The marginal density over  $z \in \mathcal{Z}_{z^*}^i$  is a standard Gaussian  $\mathcal{N}(z_i; 0, 1)$ . The marginal density  $p_{f,z^*}^i(x) = |s^i|^{-1} p(z_i)$  over  $x = f(z) \in \mathcal{M}_{f,z^*}^i$  is not Gaussian in general since  $s^i$  can vary arbitrarily over  $x \in \mathcal{M}_{f,z^*}^i$ .

[Theorem 4.12](#) addresses the key question of how column-orthogonality in the Jacobian of a VAE decoder, as promoted by diagonal variances, relates to disentanglement. Column-orthogonality of the Jacobian means that its right singular vectors are standard basis vectors that define paths in  $\mathcal{Z}$ , over which marginal densities are independent (as a property of  $p(z)$ ), such paths map to paths in  $\mathcal{X}$  over which marginal densities retain independence and factorise the density in  $\mathcal{X}$ . As in the linear case, samples generated by changing a single variable  $z_i$  will vary only in the  $i^{\text{th}}$  component of  $x = f(z)$ .

The contribution of column-orthogonality to disentanglement can be seen as twofold: (i)  $V_z$  is made constant  $\forall z \in \mathcal{Z}$  so paths  $\mathcal{V}^i$  are straight lines over which, for Gaussian  $p(z)$ , marginal densities are independent; and (ii) right singular vectors are standard basis vectors so latent variables  $z_i$  map to independent components. Note that if  $V_z$  were an arbitrary orthogonal matrix (constant  $\forall z \in \mathcal{Z}$ ), independent lines in  $\mathcal{Z}$  would still map to independent components in  $\mathcal{X}$ , but would not be axis-aligned and varying a latent variable  $z_i$  would likely change multiple components.

[Corollary 4.11](#) showed that a linear model is identifiable up to specific symmetries. Identifiability is of key interest in the non-linear case. Previously, for a sufficiently flexible Gaussian VAE  $\mathcal{G}$  with decoder  $d_{\mathcal{G}}$  trained on samples  $x \sim p(x)$  where  $p(x)$  is of the same model class (with ground truth decoder  $d$  and  $\sigma$ ), the model distribution  $p_{\mathcal{G}}(x)$  is expected to approximate  $p(x)$  (since maximising the ELBO minimises the KL divergence). From [Theorem 4.12](#) we now know that under certain conditions  $p(x)$  factorises along hidden seams following independent components. For example, for images these could be submanifolds formed by changing hair colour, object orientation or lighting. Further, if  $\mathcal{G}$  has diagonal posterior covariances,  $d_{\mathcal{G}}$  is encouraged to map latent variables to distinct components that factorise  $p_{\mathcal{G}}(x)$ . A key question is whether such model factors match those of ground truth  $p(x)$ , or if another factorisation is possible. We have proved that  $p_{\mathcal{G}}(x)$  finds ground truth factors in the linear case and conjecture that this holds in the non-linear case, but a proof is left to future work.

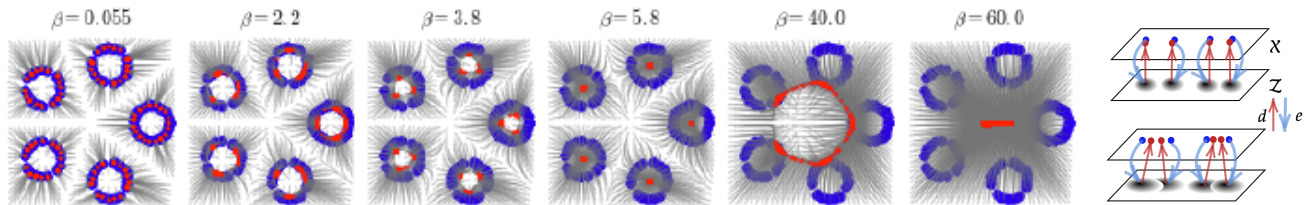


Figure 4. Effect of  $\text{Var}[x|z]$ , or  $\beta$ , on reconstruction (blue = data, red = reconstruction): (l) For low  $\beta$  ( $\beta=0.55$ ),  $\text{Var}[x|z]$  is low, by Eq. 6 & 10, and data are closely reconstructed (see right, top). As  $\beta$  increases,  $\text{Var}[x|z]$  and so  $\text{Var}[z|x]$  increase and posteriors of nearby data points  $\{x_i\}$  increasingly overlap (see right, bottom). For  $z$  in overlap of  $\{q(z|x_i)\}$ , the decoder  $\mathbb{E}[x|z]$  maps to a weighted average of  $\{x_i\}$ . Initially, close neighbours map to their mean ( $\beta = 2.2, 3.8$ ), then small circles “become neighbours” and map to their centroids, until finally all samples map to the global centroid ( $\beta = 60$ ). (reproduced with permission from Rezende & Viola, 2018) (r) illustrating posterior overlap, (t) low  $\beta$ , (b) higher  $\beta$ .

## 5. Interpreting $\beta$ of $\beta$ -VAE

We now consider the role of  $\beta$  in the  $\beta$ -VAE objective (Eq. 1), which is found empirically to affect disentanglement (Higgins et al., 2017; Burgess et al., 2018). Previous works interpret  $\beta$  as re-weighting the KL and reconstruction components of the ELBO, or serving as a Lagrange multiplier for a KL “constraint”. Here, we provide an interpretation more in keeping with the original ELBO.

To model data from a given domain, a ( $\beta$ -)VAE requires a suitable likelihood  $p_\theta(x|z)$ , e.g. a Gaussian likelihood for coloured images, and a Bernoulli for black and white images where pixel values  $x^k \in [0, 1]$  are bounded (Higgins et al., 2017). In the Gaussian case, dividing Eq. 1 by  $\beta$  shows that training a  $\beta$ -VAE with encoder variance  $\text{Var}[x|z] = \sigma^2$  is equivalent to a VAE with  $\text{Var}[x|z] = \beta\sigma^2$  and adjusted learning rate (Lucas et al., 2019). We now interpret  $\beta$  for other likelihoods.

In the Bernoulli example above, black and white image pixels are not strictly black or white ( $x^k \in \{0, 1\}$ ) and may lie between ( $x^k \in [0, 1]$ ), hence the Bernoulli distribution appears invalid as it does not sum to 1 over the domain of  $x^k$ . That is, unless each sample is treated as the mean  $\bar{x}$  of multiple (true) Bernoulli samples. Multiplying the likelihood by a factor  $\kappa > 1$  is then tantamount to scaling the number of observations as though each were made  $\kappa$  times, lowering the variance of the “mean” observation,  $\text{Var}[\bar{x}] \xrightarrow{\kappa \rightarrow \infty} 0$ .<sup>7</sup> Thus, multiplying the KL term by  $\beta$  in a  $\beta$ -VAE, or equivalently dividing the likelihood by  $\beta$ , amounts to scaling the likelihood’s variance by  $\beta$ , just as in the Gaussian case: **higher  $\beta$  corresponds to lower  $\kappa$  (“fewer observations”) and so higher likelihood variance**. Since the argument holds for any exponential family likelihood, we have proved

**Theorem 5.1** ( $\beta$ -VAE $_{\sigma^2} \equiv$  VAE $_{\beta\sigma^2}$ ). *If the likelihood  $p_\theta(x|z)$  is of exponential family form, a  $\beta$ -VAE with*

<sup>7</sup>A mode-parameterised Beta distribution could also be considered, but we keep to a more general argument.

$\text{Var}[x|z] = \sigma^2$  is equivalent to a VAE with  $\text{Var}[x|z] = \beta\sigma^2$ .

In the most general case, the  $\beta$ -ELBO (Eq. 1) is maximised if  $q(z|x) \propto p_\theta(x|z)^{1/\beta} p(z)$ , and  $\beta$  can be interpreted as a *temperature* parameter: high  $\beta$  dilates the likelihood towards a uniform distribution (high  $\text{Var}[x|z]$ ), low  $\beta$  concentrates it towards a delta distribution (low  $\text{Var}[x|z]$ ).

Figure 4 (left), from Rezende & Viola (2018), clearly illustrates the effect of varying  $\beta$  and empirically demonstrates the relationship to  $\text{Var}[x|z]$ . As variance increases, posteriors of nearby data points  $\{x_i\}$  (blue) increasingly overlap (by Eqs. 6 and 10) and the decoder maps latents in regions of overlap to weighted averages of  $x_i$  (red). Since  $\text{Var}[x|z]$  governs how close data points need to be for this effect, it acts as a “glue” over  $x \in \mathcal{X}$  (see caption for details).

In §3, we saw that optimising the ELBO encourages Jacobian orthogonality (needed for disentanglement) *in expectation* over posteriors (Eq. 8). We conjecture that this justifies why increased  $\beta$  enhances disentanglement (Higgins et al., 2017; Burgess et al., 2018): increasing  $\beta$  increases  $\text{Var}[x|z]$  and so  $\text{Var}[z|x]$  (Eq. 8), which (i) encourages orthogonality over a broader region of  $\mathcal{Z}$ ; and (ii) increases posterior overlap where multiple orthogonality constraints apply simultaneously (Fig. 4).

We note that Theorem 5.1 also allows clearer interpretation of other works that vary  $\beta$ . While setting  $\beta > 1$  can enhance disentanglement, setting  $\beta < 1$  is found to mitigate “posterior collapse” (PC), which describes when a VAE’s likelihood is sufficiently expressive such that it learns to directly model the data distribution,  $p(x|z) = p(x)$ , leaving latent variables redundant (Bowman et al., 2015).

**Corollary 5.2** ( $\beta < 1$ ). *Setting  $\beta < 1$  is expected to mitigate posterior collapse.*

*Proof.* From Theorem 5.1,  $\beta < 1$  reduces  $\text{Var}[x|z]$ , constraining the distributional family that  $p_\theta(x|z)$  can describe. For some  $\beta$ ,  $\text{Var}[x|z] < \text{Var}[x]$  and so  $p(x) \neq p_\theta(x|z)$ ,  $\forall \theta$ , making PC impossible.  $\square$



## 6. Related Work

Many works study aspects or variants of VAEs, or disentanglement in other modelling paradigms. Here, we review those that offer insight into understanding the underlying cause of disentanglement in VAEs. Higgins et al. (2017) first showed that disentanglement is enhanced by increasing  $\beta$  in Eq. 1, and Burgess et al. (2018) hypothesised that diagonal posterior covariances may be the cause, encouraging latent dimensions to align with generative factors of the data. Rolinek et al. (2019) empirically showed and theoretically supported a link between diagonal posterior covariances and orthogonality in the decoder Jacobian, deemed responsible for disentanglement. Kumar & Poole (2020) simplified and generalised the argument. These works demonstrate that diagonal posteriors provide an inductive bias that breaks the rotational symmetry of an isometric Gaussian prior, sidestepping impossibility results related to independent component analysis (e.g. Locatello et al., 2019).

Several works investigate analytically tractable linear VAEs (Lucas et al., 2019; Bao et al., 2020; Koehler et al., 2022). Zietlow et al. (2021) show that disentanglement is sensitive to perturbations to the data distribution. Reizinger et al. (2022) relate the VAE objective to *independent mechanism analysis* (Gresele et al., 2021), which encourages column-orthogonality in the mixing function of ICA, similarly to that induced implicitly in the decoder of a VAE.<sup>8</sup> Ramesh et al. (2018) trace independent factors by following leading left singular vectors of the Jacobian of a GAN generator. In the opposite direction, Chadebec & Allasonnière (2022) trace manifolds in latent space by following a locally averaged metric derived from VAE posterior covariances. Pan et al. (2023) show that the data manifold is identifiable from a geometric perspective assuming Jacobian-orthogonality, which differs to our focus on statistical independence. Recently, Bhowal et al. (2024) consider the encoder/decoder dissected into linear and non-linear aspects, loosely resembling our view of the Jacobian in terms of its SVD. However, the non-linear decoder function is quite different to its Jacobian and dissecting a function into linear and non-linear components is not well defined whereas an SVD is unique.

Recently, Buchholz et al. (2022) analysed several function classes identifiable by Independent Component Analysis (ICA), including conformal maps and orthogonal coordinate transformations (OCTs) (Defs. 2 & 3, Buchholz et al., 2022). While orthogonal in aim, this work is relevant to our analysis of a decoder with column-orthogonal Jacobian, which fit the definition of an OCT (§4.3) and slightly more constrained conformal maps are proved to be identifiable in abstract via Moebius transforms. Bringing together these perspectives may be a promising direction to understand the identifiability of VAEs and the interplay between stochastic

and deterministic approaches to learning latent generative factors.

## 7. Conclusion

Unsupervised disentanglement of independent factors of the data is a fundamental aim of machine learning and significant recent progress has been made in the case of VAEs. We extend that work by showing: (i) that the relationship between diagonal posterior covariances and column-orthogonality of the decoder Jacobian can be made more precise, obviating an approximation step in prior works; (ii) that diagonal posterior covariances in a VAE cause marginal distributions over latent variables to map to marginal distributions over statistically independent components of the data; and (iii) that *disentanglement*, previously a loosely described term, corresponds to factorising the manifold distribution as a product of push-forward distributions of independent components that correspond to distinct latent variables. We also provide a novel, yet simple interpretation of  $\beta$  in a  $\beta$ -VAE, which plausibly explains why (i) increasing  $\beta$  promotes disentanglement but degrades generation quality, and (ii) decreasing  $\beta$  mitigates posterior collapse.

Neural networks are often considered too complex to explain, even though ongoing advances make their deployment in everyday applications inevitable. Improved theoretical understanding is essential to confidently take full advantage of machine learning progress in non-trivial and potentially critical systems. We hope that the work, which provides novel insight into how probability densities can be manipulated is a useful step. Interestingly, our work shows that, regardless of the model’s complexity and non-linearity, its Jacobian that transforms the density of the prior can be considered in relatively simple terms.

Not only is a better understanding of VAEs of interest in itself, VAEs are often part of the pipeline in recent diffusion models that achieve state-of-the-art generative performance (e.g. Rombach et al., 2022; Pandey et al., 2022; Yang et al., 2023; Zhang et al., 2022). Other recent works show that supervised learning (Dhuliawala et al., 2024) and self-supervised learning (Bizeul et al., 2024) can be viewed as latent variable models trained under derivatives of the ELBO, bringing together these learning paradigms with unsupervised learning of VAEs in a common mathematical language.

A limitation of our work and of current understanding more generally is that disentanglement is observed in VAEs with non-Gaussian likelihoods (Higgins et al., 2017), whereas current work, including ours, focus predominantly on the Gaussian case. We plan to address this and identifiability of VAEs in future work.

<sup>8</sup>We report further detail on this work in Appendix B.



## Impact Statement

This paper presents theoretical results whose goal is to advance theoretical understanding in the field of Machine Learning. There are many potential societal consequences of our work, none which we feel must be specifically highlighted here.

## References

- Bao, X., Lucas, J., Sachdeva, S., and Grosse, R. B. Regularized linear autoencoders recover the principal components, eventually. In *NeurIPS*, 2020.
- Bengio, Y., Courville, A., and Vincent, P. Representation learning: A review and new perspectives. In *IEEE Transactions on Pattern Analysis and Machine Intelligence*, 2013.
- Bhowal, P., Soni, A., and Rambhatla, S. Why do variational autoencoders really promote disentanglement? In *ICML*, 2024.
- Bizeul, A., Schölkopf, B., and Allen, C. A Probabilistic Model to explain Self-Supervised Representation Learning. In *TMLR*, 2024.
- Bowman, S. R., Vilnis, L., Vinyals, O., Dai, A. M., Jozefowicz, R., and Bengio, S. Generating sentences from a continuous space. In *Conference on Computational Natural Language Learning*, 2015.
- Buchholz, S., Besserve, M., and Schölkopf, B. Function classes for identifiable nonlinear independent component analysis. In *NeurIPS*, 2022.
- Burgess, C. P., Higgins, I., Pal, A., Matthey, L., Watters, N., Desjardins, G., and Lerchner, A. Understanding disentangling in  $\beta$ -vae. *arXiv preprint arXiv:1804.03599*, 2018.
- Chadebec, C. and Allasonnière, S. A geometric perspective on variational autoencoders. In *NeurIPS*, 2022.
- Dhuliawala, S., Sachan, M., and Allen, C. Variational Classification. *TMLR*, 2024.
- Goodfellow, I., Pouget-Abadie, J., Mirza, M., Xu, B., Warde-Farley, D., Ozair, S., Courville, A., and Bengio, Y. Generative adversarial nets. *NeurIPS*, 2014.
- Gresele, L., Von Kügelgen, J., Stimper, V., Schölkopf, B., and Besserve, M. Independent mechanism analysis, a new concept? In *NeurIPS*, 2021.
- Hazami, L., Mama, R., and Thurairatnam, R. Efficientvdvae: Less is more. *arXiv preprint arXiv:2203.13751*, 2022.
- Higgins, I., Matthey, L., Pal, A., Burgess, C., Glorot, X., Botvinick, M., Mohamed, S., and Lerchner, A.  $\beta$ -VAE: Learning Basic Visual Concepts with a Constrained Variational Framework. In *ICLR*, 2017.
- Kim, H. and Mnih, A. Disentangling by factorising. In *ICML*, 2018.
- Kingma, D. P. and Welling, M. Auto-encoding variational bayes. In *ICLR*, 2014.
- Koehler, F., Mehta, V., Zhou, C., and Risteski, A. Variational autoencoders in the presence of low-dimensional data: landscape and implicit bias. In *ICLR*, 2022.
- Kumar, A. and Poole, B. On Implicit Regularization in  $\beta$ -VAEs. In *ICML*, 2020.
- Kunin, D., Bloom, J., Goeva, A., and Seed, C. Loss landscapes of regularized linear autoencoders. In *ICML*, 2019.
- Locatello, F., Bauer, S., Lucic, M., Raetsch, G., Gelly, S., Schölkopf, B., and Bachem, O. Challenging common assumptions in the unsupervised learning of disentangled representations. In *ICML*, 2019.
- Lucas, J., Tucker, G., Grosse, R. B., and Norouzi, M. Don't Blame the ELBO! a Linear VAE Perspective on Posterior Collapse. In *NeurIPS*, 2019.
- Opper, M. and Archambeau, C. The variational gaussian approximation revisited. *Neural computation*, 21(3):786–792, 2009.
- Pan, Z., Niu, L., and Zhang, L. Geometric inductive biases for identifiable unsupervised learning of disentangled representations. In *AAAI*, 2023.
- Pandey, K., Mukherjee, A., Rai, P., and Kumar, A. Diffusevae: Efficient, controllable and high-fidelity generation from low-dimensional latents. In *TMLR*, 2022.
- Papadopoulos, T. and Lourakis, M. I. Estimating the jacobian of the singular value decomposition: Theory and applications. In *ECCV*, 2000.
- Ramesh, A., Choi, Y., and LeCun, Y. A spectral regularizer for unsupervised disentanglement. *arXiv preprint arXiv:1812.01161*, 2018.
- Reizinger, P., Gresele, L., Brady, J., Von Kügelgen, J., Zietlow, D., Schölkopf, B., Martius, G., Brendel, W., and Besserve, M. Embrace the gap: Vae perform independent mechanism analysis. In *NeurIPS*, 2022.
- Rezende, D. J. and Viola, F. Taming vaes. *arXiv preprint arXiv:1810.00597*, 2018.

- Rezende, D. J., Mohamed, S., and Wierstra, D. Stochastic backpropagation and approximate inference in deep generative models. In *ICML*, 2014.
- Rolinek, M., Zietlow, D., and Martius, G. Variational Autoencoders Pursue PCA Directions (by Accident). In *CVPR*, 2019.
- Rombach, R., Blattmann, A., Lorenz, D., Esser, P., and Ommer, B. High-resolution image synthesis with latent diffusion models. In *CVPR*, 2022.
- Saxe, A. M., McClelland, J. L., and Ganguli, S. Exact solutions to the nonlinear dynamics of learning in deep linear neural networks. In *ICLR*, 2014.
- Shu, R., Chen, Y., Kumar, A., Ermon, S., and Poole, B. Weakly supervised disentanglement with guarantees. In *ICLR*, 2019.
- Tipping, M. E. and Bishop, C. M. Probabilistic principal component analysis. *Journal of the Royal Statistical Society Series B: Statistical Methodology*, 61(3):611–622, 1999.
- Yang, T., Wang, Y., Lu, Y., and Zheng, N. Disdiff: unsupervised disentanglement of diffusion probabilistic models. In *NeurIPS*, 2023.
- Zhang, Z., Zhao, Z., and Lin, Z. Unsupervised representation learning from pre-trained diffusion probabilistic models. In *NeurIPS*, 2022.
- Zietlow, D., Rolinek, M., and Martius, G. Demystifying inductive biases for (beta-) vae based architectures. In *ICML*, 2021.

## A. Appendix: Proofs

### A.1. Proof of Early Lemmas

We use notation as in §4.2: for a differentiable function  $f: \mathcal{Z} \rightarrow \mathcal{X}$  ( $\mathcal{Z} \doteq \mathbb{R}^d$ ,  $\mathcal{X} \doteq \mathbb{R}^m$ ,  $m \geq d$ ),  $\mathbf{J}_z$  denotes the first derivative or Jacobian of  $f$  evaluated at  $z \in \mathcal{Z}$ .  $\mathbf{J} = \mathbf{U}\mathbf{S}\mathbf{V}^\top$  is the singular value decomposition of  $\mathbf{J}_z$ : left singular vectors are denoted by  $\mathbf{u}^i$  (column  $i$  of  $\mathbf{U}$ ), right singular vectors by  $\mathbf{v}^i$  (column  $i$  of  $\mathbf{V}$ ) and singular values by  $s^i = \mathbf{S}_{i,i}$ .<sup>9</sup> The image of  $f$  defines a manifold  $\mathcal{M}_f \subseteq \mathcal{X}$ .

**Lemma A.1.** *If  $f: \mathcal{Z} \rightarrow \mathcal{X}$  is injective and differentiable, defining the SVD of  $\mathbf{J}_{z^*}$  for any  $z^* \in \mathcal{Z}$  uniquely defines the SVD of  $\mathbf{J}_z$  for all  $z \in \mathcal{Z}$ .*

*Proof.* By conditions on  $f$ ,  $\mathbf{J}_z$  exists and is full rank  $\forall z \in \mathcal{Z}$ . Components of the SVD of any matrix  $\mathbf{M}$  are continuous w.r.t.  $\mathbf{M}$  (Papadopoulos & Lourakis, 2000). Since  $f$  is differentiable,  $\mathbf{J}_z$  is continuous, hence the SVD of  $\mathbf{J}_z$  is a continuous function of  $z$ . Let the SVD be defined at  $z^* \in \mathcal{Z}$  and  $z^{**} \in \mathcal{Z}$  be any point. Any continuous path from  $z^*$  to  $z^{**}$  defines a sequence converging to  $z^{**}$  thus, as a continuous function of  $z$ , the SVD must converge to the same limit at  $z^{**}$ .  $\square$

Lemma A.1 does not admit piece-wise linear functions (e.g. ReLU networks) and need not hold if  $f$  is continuous and differentiable almost everywhere (i.e. discontinuities have measure zero). We therefore require  $f$  to be *quasi-differentiable*.

**Definition 4.1.** A function  $f: \mathcal{Z} \rightarrow \mathcal{X}$  is *quasi-differentiable* if it is continuous and differentiable almost everywhere.

**Lemma 4.3.** *If  $f: \mathcal{Z} \rightarrow \mathcal{X}$  is injective and  $\mathbf{V}$ -continuous, defining  $\mathbf{V}_{z^*}$  for any  $z^* \in \mathcal{Z}$  uniquely defines  $\mathbf{V}_z$ ,  $\forall z \in \mathcal{Z}$ .*

*Proof.* Differentiability of  $f$  almost everywhere implies  $\mathbf{V}$  is defined and continuous almost everywhere. While  $\mathbf{J}_z$  may be discontinuous at discrete points  $z^\dagger \in \mathcal{Z}$ , its  $\mathbf{V}$  component is continuous and so converges to the same limit for all sequences in  $\mathcal{Z}$  converging to  $z^\dagger$ . Thus, defining  $\mathbf{V}$  at  $z^* \in \mathcal{Z}$  and tracing  $\mathbf{V}$  over a continuous path from  $z^*$  to any  $z \in \mathcal{Z}$  uniquely defines  $\mathbf{V}$  at  $z$ .  $\square$

Thus specifying the order of singular vectors  $\mathbf{v}^i$  at a single point  $z \in \mathcal{Z}$  specifies them everywhere and the notion of  $i^{\text{th}}$  singular vector is well-defined. We can now define paths in  $\mathcal{Z}$  that follow  $i^{\text{th}}$  right singular vector  $\mathbf{v}^i$ .

**Definition 4.4.** If  $f: \mathcal{Z} \rightarrow \mathcal{X}$  is injective and  $\mathbf{V}$ -continuous, for  $z^* \in \mathcal{Z}$ ,  $t^* \in \mathbb{R}$  let  $z^i(t^*) \doteq z^* + \int_0^{t^*} \mathbf{v}_t^i dt \in \mathcal{Z}$ , where  $\mathbf{v}_t^i$  is the  $i^{\text{th}}$  right singular vector at  $z^i(t)$ . The set  $\mathcal{V}_{z^*}^i \doteq \{z^i(t) \mid t \in \mathbb{R}\} \subseteq \mathcal{Z}$  defines the  $i^{\text{th}}$  *singular vector path*, a continuous path in  $\mathcal{Z}$  through  $z^*$  following  $i^{\text{th}}$  right singular vectors  $\mathbf{v}^i$  of  $\mathbf{J}_z$ .

**Lemma 4.5** (Data seams). *Let  $f: \mathcal{Z} \rightarrow \mathcal{X}$  be injective and  $\mathbf{V}$ -continuous with manifold  $\mathcal{M}_f \subseteq \mathcal{X}$ ,  $z^* \in \mathcal{Z}$  and  $\mathcal{V}_{z^*}^i$  the  $i^{\text{th}}$  singular vector path through  $z^*$ . The image  $\mathcal{M}_{f,z^*}^i \subseteq \mathcal{M}_f$  of  $\mathcal{V}_{z^*}^i$  under  $f$  is a path over  $\mathcal{M}_f$  through  $f(z^*)$  following left singular vectors  $\mathbf{u}^i$  of  $\mathbf{J}_z$  (see Figure 1).*

*Proof.* By the fundamental theorem of calculus, the image of  $z(t^*)$  under  $f$  is given by

$$f(z^i(t^*)) = f(z^i(0)) + \int_0^{t^*} \frac{df}{dt} dt = f(z^*) + \int_0^{t^*} \frac{df}{dz^i} \frac{dz^i}{dt} dt = f(z^*) + \int_0^{t^*} \underbrace{\mathbf{U}\mathbf{S}\mathbf{V}^\top}_{\mathbf{J}_{z^i(t)}} \mathbf{v}_t^i dt = f(z^*) + \int_0^{t^*} s_t^i \mathbf{u}_t^i dt \quad (17)$$

where  $s_t^i$  and  $\mathbf{u}_t^i$  are the  $i^{\text{th}}$  singular value and  $i^{\text{th}}$  left singular vector of  $\mathbf{J}_{z^i(t)}$ , respectively.  $\square$

**Corollary A.2.** *For linear  $f(z) = \mathbf{D}z$ ,  $z \in \mathcal{V}_{z^*}^i$  and their images under  $f$  can be parameterised*

$$z(t) = z^* + t\mathbf{v}^i \quad \text{and} \quad f(z(t)) = f(z^*) + ts^i \mathbf{u}^i.$$

*Proof.* For linear  $f(z) = \mathbf{D}z$ , since singular values and singular vectors of the Jacobian are constant  $\forall z \in \mathcal{Z}$ . From the proof of Lemma 4.5,  $z(t) = z^* + \int_0^t \mathbf{v}^i(r) dr = z^* + \mathbf{v}^i \int_0^t 1 dr = z^* + t\mathbf{v}^i$ ; and  $f(z(t)) = f(z^*) + \int_0^t s^i(r) \mathbf{u}^i(r) dr = f(z^*) + s^i \mathbf{u}^i \int_0^t 1 dr = f(z^*) + ts^i \mathbf{u}^i$ .  $\square$

<sup>9</sup>In general,  $\mathbf{U}$ ,  $\mathbf{S}$ ,  $\mathbf{V}$ ,  $\mathbf{u}^i$ ,  $\mathbf{v}^i$  and  $s^i$  depend on  $z$  similarly to  $\mathbf{J}_z$ , but we typically suppress reference to  $z$  to lighten notation.



## A.2. Proof of Theorem 4.7

**Theorem 4.7 (Linear disentanglement).** *Under A#1, for a linear function  $f : \mathcal{Z} \rightarrow \mathcal{X}$ ,  $f(z) = \mathbf{D}z$  the push-forward distribution  $p_f^\#(x)$  factorises as a product of statistically independent components in  $\mathcal{X}$ . Lines in  $\mathcal{Z}$  following right singular vectors of  $\mathbf{D}$ , corresponding to independent  $z_i$ , map to lines in  $\mathcal{X}$  following left singular vectors of  $\mathbf{D}$  corresponding to statistically independent components.*

*Proof.*

1. The linear function  $f(z) = \mathbf{D}z$  defines a manifold  $\mathcal{M}_f \subseteq \mathcal{X}$  over which the push-forward of  $p(z)$  by  $f$  has density

$$p_f^\#(x = f(z)) = p(z) |\mathbf{J}_z|^{-1} = p(z) |\mathbf{D}|^{-1} = p(z) \prod_j |s_j|^{-1}, \quad \forall z \in \mathcal{Z}. \quad (18)$$

- (a) for linear  $f$ ,  $\mathbf{J}_z = \mathbf{D}$  is constant  $\forall z \in \mathcal{Z}$ , as are its SVD components  $\mathbf{U}$ ,  $\mathbf{S}$  and  $\mathbf{V}$ .
2. For  $z^* \in \mathcal{Z}$  and  $1 \leq i \leq d$ , let  $\mathcal{V}_{z^*}^i$  be the  $i^{\text{th}}$  singular vector path (Definition 4.4),
  - (a) by 1a, each  $\mathcal{V}_{z^*}^i$  is a straight line passing through  $z^*$  parallel to  $\mathbf{v}^i$  hence  $\mathcal{V}_{z^*}^i$  are orthogonal.
  - (b) right singular vectors  $\mathbf{v}^i$  define a (global) basis for  $\mathcal{Z}$  (the  $\mathbf{V}$ -basis) and  $v \doteq \mathbf{V}^\top z$  denotes a point  $z \in \mathcal{Z}$  in the  $\mathbf{V}$ -basis, i.e. each co-ordinate of  $z$  in the  $\mathbf{V}$ -basis is defined by projecting  $z$  onto a right singular vector,  $v_i = \mathbf{v}^{i\top} z$ .
  - (c) sampling  $z \sim p(z)$  is equivalent to sampling  $v \doteq \mathbf{V}^\top z \sim p(v)$  where  $p(v) = |\frac{dv}{dz}|^{-1} p(z) = |\mathbf{V}| p(z) = p(z)$ .
  - (d) by Gaussian symmetry,  $p(v) = \prod_i p(v_i)$  where  $p(v_i) = \mathcal{N}(v_i; 0, 1)$  ( $z_i$  and  $v_i$  are independent normal r.v.s), thus

$$p_f^\#(x) = \prod_i |s_i|^{-1} p(v_i), \quad \forall z \in \mathcal{Z}. \quad (19)$$

- (e) if  $v^*$  denotes  $z^*$  in the  $\mathbf{V}$ -basis,  $\mathcal{V}_{z^*}^i$  describes all points with co-ordinates  $v_{j \neq i}^*$  fixed and  $v_i \in \mathbb{R}$ .
- (f) sampling  $v_i \sim p(v_i)$  induces a marginal distribution over  $z \in \mathcal{V}_{z^*}^i$ :  $p_{z^*}^i(z) = p(v_i = v_i) = \mathcal{N}(v_i; 0, 1)$  ( $v_i \doteq \mathbf{v}^{i\top} z$ ).
- (g) overall,  $z^*$  lies at the intersection of lines  $\{\mathcal{V}_{z^*}^i\}_i$  and  $p(z^*) = \prod_i p_{z^*}^i(z^*)$  is the product of their marginals.
3. by Lemma 4.5, the image of each  $\mathcal{V}_{z^*}^i$  under  $f$  is a submanifold  $\mathcal{M}_{f,z^*}^i \doteq \{f(z) \mid z \in \mathcal{V}_{z^*}^i\} \subseteq \mathcal{M}_f$  following respective left singular vectors  $\mathbf{u}^i$  of  $\mathbf{J}_z$ .
  - (a) for  $x = f(z) \in \mathcal{M}_{f,z^*}^i$  and  $v_i = \mathbf{v}^{i\top} z$ , the marginal density over  $\mathcal{M}_{f,z^*}^i$  is given by  $p_{f,z^*}^i(x) = |s^i|^{-1} p(v_i)$ ;  
*Proof:* for  $x \in \mathcal{M}_{f,z^*}^i$ , divide  $p_f^\#(x)$  (Eq. 19) by  $\int_{\mathcal{M}_{f,z^*}^i} p_f^\#(x) dx = \int_{\mathcal{V}_{z^*}^i} \prod_j |s_j|^{-1} p(v_j) dv_j = \prod_{j \neq i} |s_j|^{-1} p(v_j)$ .
  - (b) each  $p_{f,z^*}^i(x)$  over  $\mathcal{M}_{f,z^*}^i$  is the push-forward of  $p_{z^*}^i(z)$  over  $\mathcal{V}_{z^*}^i$  under  $f$  restricted to its image;  
*Proof:* let  $f_{z^*}^i : \mathcal{V}_{z^*}^i \rightarrow \mathcal{M}_{f,z^*}^i$ ,  $z^i(t) \mapsto f(z^i(t))$  be such a restricted  $f$  (from a 1-D manifold to a 1-D manifold) with  $z^i(t)$  as in Definition 4.4. The marginal over  $z \in \mathcal{V}_{z^*}^i$  is given by  $p_{z^*}^i(z) = p(v_i)$  and the Jacobian of  $f_{z^*}^i$  is  $|\frac{df^i}{dz}| = |\frac{df(z^i(t))}{dt}| / |\frac{dz^i(t)}{dt}| = |s^i \mathbf{u}^i(t)| / |\mathbf{v}^i(t)| = |s^i(t)|$ , thus the marginal over  $\mathcal{M}_{f,z^*}^i$  is  $p_{f,z^*}^i(x) = |\frac{df^i}{dz}|^{-1} p_{z^*}^i(z) = |s^i|^{-1} p(v_i)$ .
  - (c) by 3a,  $p_{f,z^*}^i(x)$  are functions of distinct independent latent variables  $z_i$ , hence are *independent*.
  - (d)  $\forall z \in \mathcal{Z}$ ,  $x = f(z) \in \mathcal{M}_f$ , Eq. 18 can now be written

$$p_f^\#(x) = \prod_i p_{f,z^*}^i(x) \quad (20)$$

showing that the push-forward distribution  $p_f^\#(x)$  over  $\mathcal{M}_f$  factorises as a product of independent component distributions defined by marginal densities over submanifolds  $\mathcal{M}_{f,z^*}^i$  that pass through  $x$  following left singular vectors of  $\mathbf{J}_z$  (analogous to 2g). Each  $\mathcal{M}_{f,z^*}^i$  is the image of a line  $\mathcal{V}_{z^*}^i$  through  $z$  following right singular vectors of  $\mathbf{J}_z$ .

□

The above proof is deliberately abstract to aid generalisation to the non-linear case. Below, we define terms explicit for clarity.

1.  $\mathcal{V}_z^i \subseteq \mathcal{Z}$  are lines parallel to right singular vectors  $\mathbf{v}^i$  of  $\mathbf{D}$ . Their images  $\mathcal{M}_{f,z^*}^i \subseteq \mathcal{X}$  are parallel to left singular vectors  $\mathbf{u}^i$ . [Corollary A.2](#) gives parametrisations  $\mathcal{V}_z^i = \{z^* + t\mathbf{v}^i \mid t \in \mathbb{R}\}$  and  $\mathcal{M}_{f,z^*}^i = \{f(z^*) + ts^i\mathbf{u}^i \mid t \in \mathbb{R}\}$ .
2. The marginal distribution over  $z \in \mathcal{V}_z^i$  is  $p(z) = \mathcal{N}(v_i; 0, 1)$  where  $v_i \doteq \mathbf{v}^{i\top}z$ .
3. The marginal distributions over  $x = \mathbf{D}z \in \mathcal{M}_{f,z^*}^i$  is defined

$$p_{f,z^*}^i(x) = |s^i|^{-1}p(v_i) = |s^i|^{-1}\mathcal{N}(v_i; 0, 1) = |s^i|^{-1}\mathcal{N}(|s^i|^{-1}\mathbf{u}^{i\top}x; 0, 1) = \mathcal{N}(x^\top\mathbf{u}^i; 0, (s^i)^2).$$

where we have used  $|s^i|^{-1}\mathbf{u}^{i\top}x = |s^i|^{-1}\mathbf{u}^{i\top}(\mathbf{D}z) = |s^i|^{-1}\mathbf{u}^{i\top}(\mathbf{USV}^\top)z = \mathbf{v}^{i\top}z = v_i$ .

4. The push-forward distribution over the mean manifold is given by

$$\begin{aligned} p(x) &= \mathcal{N}(x; 0, \mathbf{D}\mathbf{D}^\top) = (2\pi)^{-d/2}|\mathbf{D}\mathbf{D}^\top|^{-1/2} \exp\left\{-\frac{1}{2}x^\top(\mathbf{D}\mathbf{D}^\top)^{-1}x\right\} \\ &= (2\pi)^{-d/2}|\mathbf{S}^2|^{-1/2} \exp\left\{-\frac{1}{2}x^\top\mathbf{U}\mathbf{S}^{-2}\mathbf{U}^\top x\right\} \\ &= \left(\prod_i (2\pi(s^i)^2)^{-1/2}\right) \exp\left\{-\frac{1}{2}\sum_i (s^i)^{-2}(\mathbf{u}^{i\top}x)^2\right\} \\ &= \prod_i (2\pi(s^i)^2)^{-1/2} \exp\left\{-\frac{1}{2(s^i)^2}(\mathbf{u}^{i\top}x)^2\right\} = \prod_i \mathcal{N}(\mathbf{u}^{i\top}x; 0, (s^i)^2) \end{aligned}$$

Step 4 shows that the distribution over the manifold factorises and step 3 shows that its factors, or components, are independent and defined by push-forward distributions of independent latent variables. Note that the explicit analytical form for component distributions in step 3 is specific to the linear case and cannot be defined in general.

### A.3. Proof of [Corollary 4.11](#)

**Corollary 4.11 (LVAE identifiability).** *For  $n$  data samples generated under the model in [Eq. 2](#) (PPCA model), in the limit  $n \rightarrow \infty$ , an LVAE identifies statistically independent components of the data and the decoder maps latent variables to distinct components. If singular values of ground truth  $\mathbf{D}$  are distinct, the model is uniquely identified (up to permutation and sign).*

*Proof.* As stated previously, the noise parameter  $\sigma$  is assumed to be learned (as in PPCA, [Tipping & Bishop, 1999](#)) or otherwise well-approximated.

- For  $n$  data samples from the PPCA model ([Eq. 2](#)) with ground truth parameter  $\mathbf{D} = \mathbf{USV}^\top$ , as  $n \rightarrow \infty$ , the empirical distribution tends to  $\mathcal{N}(x; 0, \mathbf{D}\mathbf{D}^\top + \sigma^2\mathbf{I})$  and for an optimised LVAE  $\mathbf{D}_{\text{LVAE}} \rightarrow \mathbf{US}$ .
- The PPCA model satisfies conditions of [Theorem 4.7](#) ( $f$  linear,  $p(z)$  standard Gaussian), therefore paths following ground truth left singular vectors  $\mathbf{u}^i$  correspond to independent components of the distribution over mean parameters  $\mu = \mathbf{D}z$ ,  $z \sim p(z)$ , i.e. marginal distributions over such paths are independent and factorise  $p(\mu)$ .
- In the limit  $n \rightarrow \infty$ , an LVAE learns ground truth singular vectors  $\mathbf{u}_i$  and so identifies independent components of the data.
- In the limit  $n \rightarrow \infty$ , right singular vectors  $\mathbf{v}^i$  of  $\mathbf{D}_{\text{LVAE}}$  are standard basis vectors ( $\mathbf{V} = \mathbf{I}$ ). Thus by [Lemma 4.5](#), varying co-ordinate  $z_i$  of any  $z^* \in \mathcal{Z}$  (i.e. following  $\mathcal{V}_{z^*}^i$  in  $\mathcal{Z}$ ), corresponds to following the  $i^{\text{th}}$  left singular vector  $\mathbf{u}^i$  from  $f(z^*) \doteq \mathbf{D}_{\text{LVAE}}z^*$  (i.e. following  $\mathcal{M}_{f,z^*}^i$  in  $\mathcal{X}$ ).<sup>10</sup> Thus, varying  $z_i$  in  $\mathcal{Z}$  varies the  $i^{\text{th}}$  independent component in  $\mathcal{X}$ .
- If  $s^i$  are distinct, the SVD of  $\mathbf{D}$  is unique up to column permutation and sign, hence  $\mathbf{D}$  is identifiable up to the same symmetry. □

<sup>10</sup>For linear  $f$ , this can be seen explicitly:  $\mathbf{D}_{\text{LVAE}}(z^* + tz^i) = \mathbf{D}_{\text{LVAE}}z^* + t\mathbf{u}^i$ , ( $t, t' \in \mathbb{R}$ ).

#### A.4. Proof of Theorem 4.12

**Theorem 4.12 (Non-linear disentanglement).** *Under A#1-3, the push-forward distribution  $p_f^\#$  factorises as a product of statistically independent components in  $\mathcal{X}$  (Eq. 16). Lines in  $\mathcal{Z}$  following standard basis vectors corresponding to independent latent variables are mapped to sub-manifolds in  $\mathcal{X}$  following left singular vectors of the Jacobian  $\mathbf{J}_z$  that correspond to statistically independent components.*

*Proof.*

1.  $f$  defines a manifold  $\mathcal{M}_f \subseteq \mathcal{X}$  over which the push-forward of  $p(z)$  by  $f$  has density

$$p_f^\#(x=f(z)) = p(z)|\mathbf{J}_z|^{-1} = p(z) \prod_j |s_j|^{-1} = \prod_j |s_j|^{-1} p(z_i), \quad \forall z \in \mathcal{Z}. \quad (21)$$

- (a) by A#3,  $\mathbf{J}_z = \mathbf{U}_z \mathbf{S}_z \mathbf{V}_z^\top$  where  $\mathbf{V}_z = \mathbf{I}, \forall z \in \mathcal{Z}$ , i.e. the right singular vectors of  $\mathbf{J}_z$  are standard basis vectors  $\mathbf{z}^i$ .
2. For  $z^* \in \mathcal{Z}$  and  $1 \leq i \leq d$ , let  $\mathcal{V}_{z^*}^i$  be the  $i^{\text{th}}$  singular vector path (Definition 4.4),
  - (a) by 1a, each  $\mathcal{V}_{z^*}^i$  is a straight line passing through  $z^*$  parallel to standard basis vector  $\mathbf{z}^i$ .
  - (b)  $z^*$  lies at the intersection of lines  $\{\mathcal{V}_{z^*}^i\}_i$  and  $p(z^*) = \prod_i p(z_i^*)$  is the product of their marginals.
3. by Lemma 4.5, the image of each  $\mathcal{V}_{z^*}^i$  under  $f$  is a submanifold  $\mathcal{M}_{f,z^*}^i = \{f(z) \mid z \in \mathcal{V}_{z^*}^i\} \subseteq \mathcal{M}_f$  following respective left singular vectors  $\mathbf{u}^i$  of  $\mathbf{J}_z$ .
  - (a) for  $x = f(z) \in \mathcal{M}_{f,z^*}^i$ , the marginal density over  $\mathcal{M}_{f,z^*}^i$  is given by  $p_{f,z^*}^i(x) = |s^i|^{-1} p(z_i)$ ;  
*Proof:* for  $x \in \mathcal{M}_{f,z^*}^i$ , divide  $p_f^\#(x)$  (Eq. 21) by  $\int_{\mathcal{M}_{f,z^*}^i} p_f^\#(x) dx = \int_{\mathcal{V}_{z^*}^i} \prod_j |s_j|^{-1} p(z_j) dz_i = \prod_{j \neq i} |s_j|^{-1} p(z_j)$ .
  - (b)  $p_{f,z^*}^i(x)$  over  $\mathcal{M}_{f,z^*}^i$  is the push-forward of  $p_{z^*}^i(z)$  over  $\mathcal{V}_{z^*}^i$  under  $f$  restricted to its image;  
*Proof:* let  $f_{z^*}^i : \mathcal{V}_{z^*}^i \rightarrow \mathcal{M}_{f,z^*}^i$ ,  $z^i(t) \mapsto f(z^i(t))$  be such a restricted  $f$  (from a 1-D manifold to a 1-D manifold) with  $z^i(t)$  as in Definition 4.4. The marginal over  $z \in \mathcal{V}_{z^*}^i$  is given by  $p_{z^*}^i(z) = p(z_i)$  and the Jacobian of  $f_{z^*}^i$  is  $|\frac{df^i}{dz}| = |\frac{df(z^i(t))}{dt}| / |\frac{dz^i(t)}{dt}| = |s^i \mathbf{u}^i(t)| / |\mathbf{v}^i(t)| = |s^i(t)|$ , thus the marginal over  $\mathcal{M}_{f,z^*}^i$  is given by  $p_{f,z^*}^i(x) = |\frac{df^i}{dz}|^{-1} p(z_i) = |s^i|^{-1} p(z_i)$ .
  - (c) by 3a,  $p_{f,z^*}^i(x)$  are functions of distinct independent latent variables  $z_i$ , hence are *independent*.
  - (d)  $\forall z \in \mathcal{Z}$ ,  $x = f(z) \in \mathcal{M}_f$ , Eq. 18 can now be written

$$p_f^\#(x) = \prod_i p_{f,z^*}^i(x) \quad (22)$$

showing that the push-forward distribution  $p_f^\#(x)$  over  $\mathcal{M}_f$  factorises as a product of independent component distributions defined by marginal densities over submanifolds  $\mathcal{M}_{f,z^*}^i$  that pass through  $x$  following left singular vectors of  $\mathbf{J}_z$  (analogous to (2b)). Each  $\mathcal{M}_{f,z^*}^i$  is the image of a line  $\mathcal{V}_{z^*}^i$  in  $\mathcal{Z}$  passing through  $z$  parallel to standard basis vectors (i.e. axis-aligned).  $\square$

## B. Material Errors in (Reizinger et al., 2022)

We note what appear to be several fundamental mathematical errors in the proof of Theorem 1 in (Reizinger et al., 2022) rendering it invalid. Theorem 1 claims an approximation to the exact relationship given in Equation (8)

- p.33, after ‘‘triangle inequality’’:  $|\mathbb{E}[\|a\|^2 - \|b\|^2]| \leq \mathbb{E}[\|a - b\|^2]$ , where  $a = x - f$ ,  $b = -\sum \frac{\partial f}{\partial z_k} \dots$ 
  - (dropping expectations for clarity) this has the form  $|\|a\|^2 - \|b\|^2| \leq \|a - b\|^2$  (\*)
  - true triangle inequality:  $\| \|a\| - \|b\| \| \leq \|a - b\| \implies \| \|a\| - \|b\| \|^2 \leq \|a - b\|^2$  (by squaring)
    - \* this differs to (\*) since norms are squared inside the absolute operator on the left hand side.
  - counter-example to (\*):  $b = x > 0$ ,  $a = x + 1 \implies \| \|a\|^2 - \|b\|^2 \| = |2x + 1| > 1 = \|a - b\|^2$
- next step, p.33:  $\mathbb{E}[\|(c-e) - (d-e)\|^2] \leq \mathbb{E}[\|c-e\|^2 + \|d-e\|^2]$  where  $c = x$ ,  $d = f(z) - \sum \frac{\partial f}{\partial z_k} \dots$ ,  $e = f(\mu)$



## Unpicking Data at the Seams

---

- this has the form of the standard triangle inequality  $\|a-b\| \leq \|a\| + \|b\|$  except all norms are squared
- squaring both sides of the triangle inequality gives an additional cross term on the right that the used inequality omits, without which the inequality does not hold in general
- first step, p.34: drops the  $K$  term, which bounds the decoder Hessian and higher derivatives (in earlier Taylor expansion)
  - this omission is similar to a step in (Kumar & Poole, 2020) but is not justified in the paper, e.g. in Assumption 1.
  - since  $K$  is unbounded, any conclusion omitting it without justification is not valid in general